Solvation Dynamics in Biological Systems and Organized Assemblies

Pratik Sen,[a] Subrata Pal,[b] Kankan Bhattacharyya[a]* and Biman Bagchi[b]*
[a]*Department of Physical Chemistry, Indian Association for the Cultivation of Science, Jadavpur, Kolkata 700 032, India*
[b]*Solid State and Structural Chemistry Unit, Indian Institute of Science, Bangalore 560 012, India*

Solvation dynamics of a polar probe in many biological systems and organized assemblies displays a surprising ultraslow component. The origin of this anomalous ultraslow component is investigated using experiments, theory and computer simulations. We first summarize some recent experimental results on solvation dynamics, e.g., temperature dependence, site dependence at active site of an enzyme and red edge excitation shift (REES). Then we propose two new theoretical models to explain the ultraslow component. The first one involves the motion of the 'buried water' molecules (both translation and rotation) accompanied by cooperative relaxation ('local melting') of several surfactant chains. An estimate of the time is obtained by using an effective Rouse chain model of chain dynamics, coupled with a mean first passage time calculation. The second explanation invokes self-diffusion of the (di)polar probe (created by optical excitation) *itself* from a less polar to a more polar region. This may also involve cooperative motion of the surfactant chains in the hydrophobic core, if the probe has a sizeable distribution inside the core prior to excitation. It may also involve escape of the probe to the bulk from the surface of the self-assembly. The second mechanism should result in the *narrowing of the full width of the emission spectrum with time*, which has indeed been observed in recent experiments. It is argued that both the two mechanisms may give rise to an ultraslow time constant and may be applicable to different experimental situations. The effectiveness of solvation as a dynamical probe in such complex systems has been discussed. Finally, we give a brief overview of recent results on computer simulations on dynamics of water molecules around a protein and a micelle.

Keywords: Solvation dynamics; Biological water; Micelles; Proteins; Emission spectrum.

INTRODUCTION

In recent years, time dependent Stokes shift of fluorescence (TDFSS) studies of a probe dye molecule has provided a wealth of information on dynamics of dipolar liquids, particularly water.[1-3] In these experiments, a sudden (instantaneous) change in the charge distribution of the probe molecule is created optically using an ultrashort laser pulse. Subsequent change in the energy of the probe solute is monitored through the fluorescence frequency of the probe. Solvation time correlation function is defined as[1-3]

$$S(t) = \frac{\nu(t) - \nu(\infty)}{\nu(0) - \nu(\infty)} \quad (1)$$

where ν(t) is the average frequency at a time t of the fluorescence spectrum from the probe molecule. S(t) evolves from unity at time t = 0 to zero as time goes to infinity. The time dependence of S(t) describes in detail the time dependent response of the liquid to the sudden change in the charge distribution in the probe (solute). Since energy derives contributions from interactions with many solvent molecules, this response is collective. If the perturbation is small, the dynamics described by S(t) is expected to be equivalent to the decay of the *equilibrium* time correlation function, C(t), which is given by

$$C(t) = \frac{< \delta E_{solv}(0) \delta E_{solv}(t) >}{< \delta E_{solv}(0) \delta E_{solv}(0) >} \quad (2)$$

where $\delta E_{solv}(t)$ is the fluctuation in the solvation energy about the equilibrium solvation energy. Detailed knowledge of the time dependence of C(t) is of fundamental importance to understand solvent effects in many chemical

Special Issue for the 4th Asia Photochemistry Conference, January 5~10, 2005, Taipei, Taiwan, R.O.C.
* Corresponding author. Fax: 91-33-2473-2805; E-mail: pckb@mahendra.iacs.res.in

processes, such as electron transfer or dephasing.

Solvation dynamics in liquid water have attracted special attention for the ubiquitous role of water in biology.[1-7] Solvation dynamics in pure water shows ultrafast solvation, with the initial component in the few tens of femtoseconds. In bulk water, even the slowest component is only about 1 ps.[1-7] However, in a biological or an organized assembly, the long component of solvation dynamics slows down quite dramatically.[8-14] At the surface of a protein, solvation dynamics displays a component which is slower by one to two orders of magnitude compared to bulk water and the ultraslow component ranges from a few tens to a few hundreds of picoseconds.[8-10] The ultraslow component in a cyclodextrin cavity is nearly 1000 times slower than that in bulk water.[11] In the case of solvation dynamics in DNA,[12] proteins, aqueous polymer solutions, micelles, and reverse micelles a definite ultraslow component even greater than 1 ns (1000 ps) has been observed.[5-7]

In this article, we first briefly review the recent experimental results on solvation dynamics in biological and organized assemblies. We then propose two new theoretical models. Finally, we will give a brief outline of some recent results of computer simulations.[15-20]

RECENT EXPERIMENTAL RESULTS

Solvation Dynamics at the Active Site of an Enzyme

One of the longstanding goals of enzymology is to elucidate the physical origin of the extraordinary specificity of an enzyme, i.e., molecular recognition. It is proposed that the active site of an enzyme is pre-organized. We addressed the question of whether the water molecules at the active sites are also pre-organized and what happens if a charged or highly polar substrate approaches an enzyme. For this purpose, we labeled an enzyme glutaminyl t-RNA synthetatse (GlnRS) with a solvation probe acrylodan.[24] The biological function of this enzyme is to bind to an amino acid glutamine (Gln) and t-RNA so that Gln is attached to and carried by t-RNA for protein synthesis. The decay of C(t) of wild GlnRS in free form and that in GlnRS bound to Gln and t-RNA are shown in Fig. 1.[24] We found that in the free enzyme (GlnRS), the solvation dynamics displays two components of 400 ps and 2000 ps.[24] When Gln binds to GlnRS the 400 ps component is lengthened to 750 ps while the 2000 ps component remains unchanged. However, when t-RNA binds to GlnRS, the 400 ps component remains unaffected but the 2000 ps component becomes slower (2500 ps). This suggests the dynamics of the water molecules at the Gln binding site (400 ps) and that at the t-RNA binding site (2000 ps) are different. The presence of the slow water molecules at the active site seems to be highly beneficial because if the response of the water molecules was too fast that could lead to drastic change of the hydration layer and hence, structure of a protein when a polar substrate approaches it. Thus it seems that presence of slow water molecules at the active site is essential for enzyme catalysis.

Another important issue is what happens to the dynamics of the water molecules in a hydration shell of a non-native state of a protein. To investigate this, we have studied solvation dynamics in GlnRS in a molten globule state,[25] in a protein (lysozyme) denatured by SDs and a mercaptanol.[26] Lysozyme denatured by urea may be refolded by the addition of a small amount of the surfactant (SDS). We have investigated this phenomenon using solvation dynamics.[27] In all cases, it is observed that even in the biologically inactive state there are an appreciable number of slow water molecules around the protein. Many proteins and other biological assemblies may be stored in the nanoporous sol-gel glass for a long time. Such a glass doped with organic systems is called an ormosil. We have recently studied dynamics in this emerging material.[28]

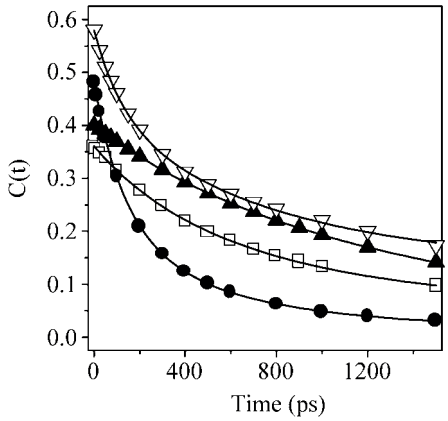

Fig. 1. Decay of C(t) of acrylodan labeled (i) mutant Y211H GlnRS (▽); (ii) GlnRS with glutamine (▲); (iii) wild-type GlnRS (□) and (iv) wild-type GlnRS with t-RNA^{gln} and ATP (•). The points denote the actual values of C(t) and the solid line denotes the best fit to an exponential decay (ref. 24).

Excitation Wavelength Dependence of Solvation Dynamics in Reverse Micelles and Lipids

In an organized assembly, the local polarity or the dielectric constant of the confined water molecules varies strongly over distance from the polar head groups. The variation of the local dielectric constant in an inhomogeneous medium gives rise to the red edge excitation shift (REES). REES refers to red shift of the emission maximum with increase in excitation wavelength. The fundamental basis of REES is, if a fluorescent probe is distributed over the entire organized assembly (from highly non-polar surfactant chains to highly polar water), the absorption maximum is different in different regions. Thus by varying excitation wavelength one can selectively excite probes in different regions and thus, dynamics in different regions of an organized assembly. Using this principle, we been successful to spatially resolve solvation dynamics in a reverse micelle[29] and in a lipid.[30] We found that the longer is the excitation wavelength the faster is the dynamics. As an example, excitation wavelength dependence of the solvation dynamics in a lipid is shown in Fig. 2.

Temperature Dependence of Solvation Dynamics in a Micelle

Nanndi and Bagchi earlier proposed a model involving dynamic equilibrium between free and bound water molecules in the vicinity of a biological macromolecule.[8] According to this model, the slow component of relaxation depends on the binding energy, i.e. free energy difference (ΔG_{bf}^{0}) between bound and free water. In the limit of high binding energy ($k_{fb} >> k_{bf}$) the time constant for the slowest component is given by

$$k_{slow} \approx k_{bf}^{-1} \tag{3}$$

According to this model, the activation energy for bound-to-free interconversion is $\Delta G_{bf}^{0} + \Delta G^{\neq}$ where $\Delta G^{\neq}$ is the activation energy for free-bound interconversion.[8] In order to verify the dynamic exchange model, we studied temperature variation of solvation dynamics in a micelle (triton X100, Tx-100).[13] Fig. 3 shows solvation dynamics in TX-100 at different temperatures. From temperature variation, we found that solvation dynamics in TX-100 micelle involves an activation energy of 9 kcal mol^{-1} and a positive entropy of activation of 14 cal/mol.[13] This finding is consistent with a recent computer simulation.[16] According to a computer simulation the hydrogen bond energy of the interfacial water molecules and the polar head groups is stronger by 7-8 kcal mol^{-1} compared to bulk water.[16]

Solvation Dynamics of a Protein in a Vesicle

The ultraslow solvation may originate from overall tumbling motion of the protein or the self-assembly. Dielectric relaxation times in an aqueous solution of a protein span a wide range and may be classified as:[9] (1) reorientation of bulk water (8 ps); (2) overall tumbling or reorienta-

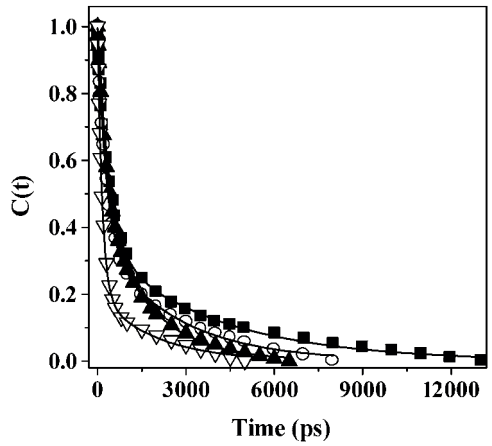

Fig. 2. Decay of response function, C(t) of C480 in DMPC vesicles for λ_{ex} = 390 nm (filled square), λ_{ex} = 400 nm (circle), λ_{ex} = 410 nm (filled triangle) and λ_{ex} = 420 nm (open triangle). The points denote the actual values of C(t) and the solid line denotes the best fit to a biexponential decay (ref. 30).

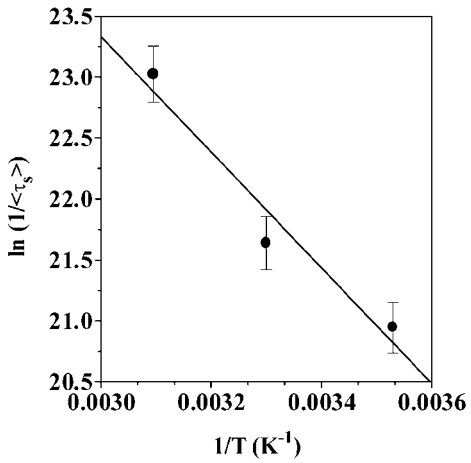

Fig. 3. Plot of ln (1/<τ_s>) against 1/T of 4-AP in 100 mM TX-100 (ref. 13).

tion of the entire protein molecule (10-100 ns) and (3) relaxation of water associated with the protein (10-150 ps). According to the Stokes-Einstein relation, the overall tumbling time (τ_m) of a biological system of volume V is given by

$$\tau_m = \eta V/k_B T \quad (4)$$

where η is the viscosity of water. From this relation, τ_m may be calculated if the volume of the macromolecule is known. The protein, human serum albumin (HSA) is ellipsoidal of dimensions 8 nm × 8 nm × 3 nm. Thus for HSA, τ_m is 25 ns in bulk water. It should be emphasized that if the probe is attached to the protein surface the overall tumbling gives rise to a relative motion of the probe and the water molecules surrounding the protein.

One way to check the role of overall tumbling is to create a situation when overall tumbling of the protein is constrained to be slow. If a protein is confined inside a water pool of the reverse micelle or a lipid the lipid vesicle or the reverse micelle tumbles as a whole. The radius (r_h) of a DMPC vesicle is about 15 nm. Thus, the volume of the vesicle is about 140 times that of a single HSA molecule. From equation (4), τ_m is 3500 ns for the lipid vesicle. Evidently, overall tumbling of the lipid vesicle (τ_m = 3500 ns) is impossible within the excited lifetime (1-2 ns) of the fluorescent probe (DCM). Wand et al.[31] demonstrated that when a protein is incorporated in the water pool of a reverse micelle, tumbling of the protein is completely eliminated and this leads to line narrowing and a sharp NMR spectra. We demonstrated that when HSA is entrapped in a DMPC vesicle the 10 ns component vanishes.[32] This suggests that overall tumbling of the protein could be a possible source for the 10 ns component.

THEORETICAL FORMULATION

In this section, we consider the role of chain dynamics and self-diffusion of probe in explaining the ultraslow component of solvation dynamics in an organized assembly.

Before we discuss the theoretical models, we emphasize that an organized assembly is heterogeneous on a mesoscopic length scale, (i.e. 30-100 Å). The equilibrium solvation energy of the charged probe is different in different phases because the polarity and the effective dielectric constant of the individual phases are different. Thus solvation energy of a polar probe inside the hydrocarbon core of a micelle is expected to be much less than that at the micelle-water interface while the latter is again smaller than that in the bulk water. For simplicity, we consider a two phase system, with water being the outer phase. We also assume that the *probe is hydrophobic in its ground state*. Therefore, it is distributed primarily at the interface and also inside the hydrophobic core. The excited state of the probe, however, is polar (dipolar or charged).

The structure of the hydration shell of many macromolecular assemblies have been studied by computer simulations and neutron scattering. According to computer simulations, in the hydration layer the macromolecules or the surfactants are connected by hydrogen bond bridges involving water molecules (water bridges).[21-23] The exact number of water bridges vary from one system to another. A single water molecule may form an intramolecular hydrogen bond bridge between two oxygen atoms of the same surfactant chain or an intermolecular hydrogen bond bridge between two neighboring surfactant molecules.[21-23] In the case of a lipid (DMPC) bilayer about 70% of the surfactant (DMPC) molecules are found to be linked by either single or multiple intermolecular water bridges.[21] In many cases, two DMPC molecules are simultaneously linked by 2, 3 and in rare cases by 4 parallel water bridges.[21] Such double or multiple hydrogen bonding gives a certain amount of stability to these water molecules. Also, the clustering of the water molecules around a macromolecule leads to close packing and a density higher (1.25 times) than that in bulk water.[15]

Model 1: Dynamics of Surfactant Chains with Buried, Slow Water

In this section, we consider the response of the buried water following creation of the dipole in terms of cooperative chain melting. Subsequent to the creation of the polarization field by the external probe near the surface, the buried water molecules inside a micelle (or in general in an organized assembly) would need to reorient to minimize the energy. The reorientation of water molecules involve rupture of the hydrogen bond of a water molecule with another water molecule or with the surfactant and reformation of a

hydrogen bond with the dipole created (Fig. 4). This involves not only breaking and formation of hydrogen bonds but also rotation and migration of water molecules inside the layer and also of "breathing" motion of the surfactant chains (Fig. 4). Dynamics of such a process is expected to be rather slow and should be related to the dynamics of the surfactant chain.

In order to estimate the time constant of the relaxation of the buried water molecules we assume the following simple model. Guided by experiments and simulations,[13,16] we assume that the water molecules need to undergo a reaction between two minima which involves an activation barrier of ~9 kcal/mole and a positive entropy factor. Next, we assume that the breakage of the hydrogen bond and its realignment or relocation requires cooperative motion of the nearest neighbor surfactant chains, (may be two in number or greater). Thus, what we propose is a local melting in the hydrophobic core (Fig. 4). We now present a quantitative estimate of the time required for such melting. Note that this will be a slow process and is expected to be the rate limiting step in the solvation energy relaxation in the hydration shell.

In order for a cooperative melting to occur, one requires phase coherence in the motion of all the neighboring chains. We model this by assuming that each monomer of the chain has locally z number of states (chain conformations). Next, one needs to estimate the size of the region that can melt cooperatively. Let us assume that this number be denoted by N. If τ_0 is the time required for transition from the ground to the excited state, then the time required for the phase coherence required for local melting is

$$\tau = z^N \tau_0 \tag{5}$$

We assume that $z = 2$, with a ground state denoted by *0* and the excited state by *1*. If we further assume that the fluorescent solvation probe is surrounded by two surfactant chains, then the *lowest size* that can melt is a cell that contains 2 monomers, that is $N = 2$. Note that this is the lowest size and this can only be larger because of the involvement of more than 2 chains. It is difficult to obtain an estimate of τ_0 from any microscopic considerations because of the complexity of interactions and the highly condensed state of the hydration layer. We thus take recourse to the Rouse chain dynamics and assume that it can provide the estimate via the largest wave number fluctuation relaxation time.

$$\tau_0 = 1/\lambda_{N-1} = (3D_0)^{-1}[Nb/(N-1)\pi]^2 \tag{6}$$

For TX-100, $N \approx 10$. We next need an estimate of D_0 which

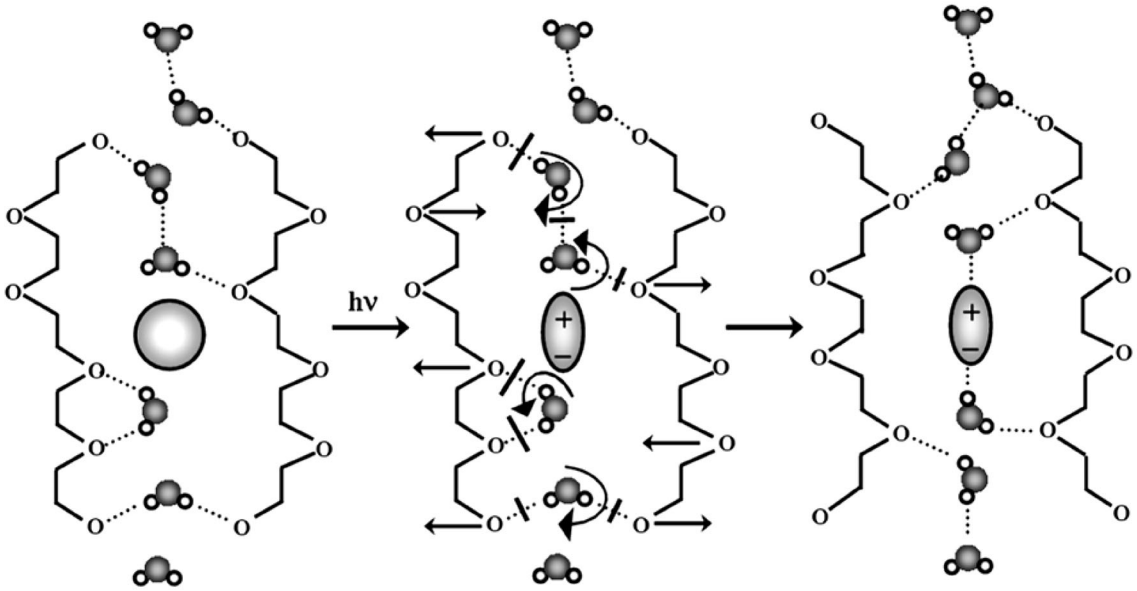

Fig. 4. A schematic illustration of the role of buried water in the solvation dynamics of a probe which is also initially located inside the self-assembly. This particular example illustrates the possible rearrangement of water molecules in a micelle of surfactant of polyethylene glycol (polyoxyethylene surfactants) subsequent to optical excitation.

we obtain by using Stokes-Einstein relation ($D_0 = kT/6\pi\eta_{eff}$ r) with an effective viscosity of the hydration layer, η_{eff} and a radius r of the monomer (C_2H_4O, in the case of a triton X-100 micelle) unit.

The logic of the above analysis is that the hydrogen bond breaking requires a local excitation of the nearby surfactants. This excitation we calculate by using the normal modes of the surfactant chains and a first passage time calculation. We assume that these normal modes remain unperturbed by the presence of the others.

The advantage of the above simple expressions is that one can now easily estimate the relaxation time. If we assume that the radius of the monomer for a TX micelle (C_2H_4O) unit is 3 Å and the effective viscosity 0.3 cP,[33] then the above expression gives a value of $\tau_0 \approx 0.5$ ns. Use of this time constant in Eq. 6 gives a value of about 2 ns for the formation of the local excited state. So, this is the approximate theoretical estimate of the ultraslow component arising from co-operative chain melting in the hydration layer. Note that the time required for hydrogen bond breaking is much smaller. It is about 10-100 ps for a single hydrogen bond and somewhat longer for the double bond which needs to be broken consecutively and which can be further slowed down by reformation.

The above estimate is certainly approximate and depends on the parameters chosen. Still we believe that we have obtained a reasonable number for the rate constant of this complex process of cooperative melting. The main features of this mechanism can be summarized as the *lengthening of time of relaxation of deeply buried water in an organized assembly (such as a triton X-100 micelle) due to a high degree of cooperation required for these water molecules to participate in the solvation dynamics.*

Model 2: Self-diffusion of the Probe

The second explanation invokes the motion of the probe itself. An organized assembly usually consists of a large hydrophobic core, and a fluorescent probe used for solvation dynamics studies is largely hydrophobic in its ground state. In the model involving self-diffusion one assumes that in the ground state a significant percentage of the probe molecules are trapped inside the relatively less polar region of the micelles/reverse micelles with a major portion of the probe inside the hydrocarbon chains. Subsequent to excitation, the dipole moment of the probe increases substantially. Thus, the excited probe tends to move to a more polar and lower energy region, i.e., the interface between bulk water and the surfactant chain (Fig. 5).

Experimentally, self-diffusion manifests in narrowing of the emission spectrum with increase in time (full width at half maxima, Γ). Recently, several groups have reported decay of Γ with time (t).[14] Qualitatively, this may explained as follows. At t = 0, the probe molecules in different environments are excited simultaneously. Due to the superposition of the emission spectra in different environments at short times, the spectral width of the emission spectrum is very large. Following electronic excitation the probe molecule becomes highly polar and hence, after excitation the probe molecules from all locations move towards the most polar region (Fig. 5). At a sufficiently long time, all the probe molecules reach the most polar region and all of them experience a more or less uniform environment. This results in a small Γ. Thus the time constant of decay of Γ may be ascribed to self-diffusion of the probe. Dutta et al. showed that in a reverse micelle, Γ(t) of DCM exhibits a decrease by as much as 70% (Fig. 6).[14] They also showed that the time constant of decay of Γ(t) of DCM is similar to that of C(t) and hence, in this case the slow solvation dynamics is attributed to self-diffusion of the probe (DCM).[14]

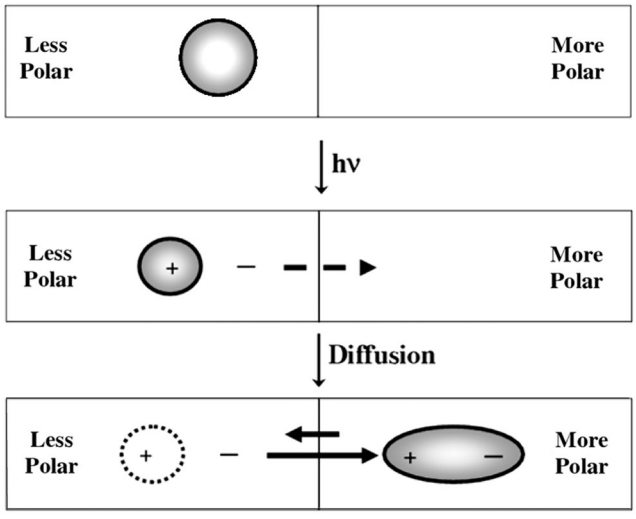

Fig. 5. A schematic illustration of creation of a dipole and subsequent diffusion following optical excitation of the probe. In the excited state, the highly polar probe undergoes diffusion from less polar to the more polar state.

It should be noted that the time dependent change in spectral width observed is observed only in selected cases. For instance, the same probe (DCM) which exhibits time dependent change in Γ in a reverse micelle does not show similar behavior when entrapped in a bile salt micelle.[14] In the latter, DCM is confined in a very long (5 nm) cylindrical water filled core. As a result, within its excited state lifetime the probe does not come out in bulk water and does not experience a large variation of local polarity.[14]

The diffusion coefficient ($D_{\|}$) of fluorescent probe for translation parallel to the surface of an organized assemble may be obtained from the fluorescence anisotropy decays using the "wobbling-in-cone" model.[34] It is observed that $D_{\|}$ is smaller than that in bulk water (~10^{-5} cm^2 s^{-1}) only by a factor of 2-5.[34] Thus the probe undergoes diffusion over a distance ($<z^2> = 2D_{\|}t$) of about 10 Å in one ns. The diffusion from non-polar to polar region is in a direction normal to the surface of a micelle (or other organized assembly) and the corresponding diffusion coefficient $D_{\perp}$ may not be equal to $D_{\|}$.

We now present a molecular theory for the above dynamical process, namely, self-diffusion in an inhomogeneous medium. A starting point for developing such a molecular theory is to use a time dependent density functional

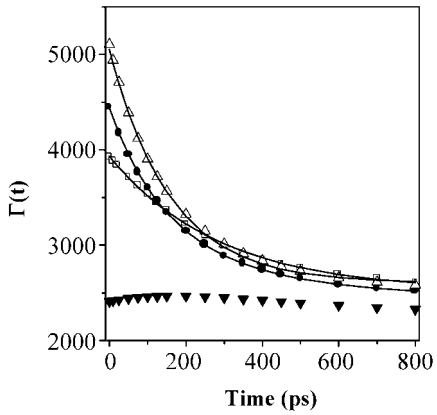

Fig. 6. The plot of full width at half maximum (FWHM, Γ) of the TRES against time of DCM in 1.5 gm AOT in 8 mL *n*-heptane at $w_0 = 39.5$ with no additives (square), with 1 mM Na-sal (filled circle), with 100 mM Na-cholate (open triangle) and of DCM in the presence of 100 mM Na-cholate in bulk water (filled triangle). The points denote the actual values of Γ and the solid line denotes the best fit to a biexponential decay (ref. 14).

theory which gives the following expression for the position (X) dependent energy of interaction of a probe with the surrounding medium

$$E(X,t) = \int dX' C_{PS_i}(X - X')\delta\rho_{S_i}(X',t) - \int dX' C_{Pw}(X - X')\delta\rho_w(X',t), \quad (7)$$

where C_{PSi} is the two particle direct correlation function between the polar probe and the ith group of the surfactant/polymer and C_{Pw} is the probe-water direct correlation function. In the inhomogeneous system, these pair correlation functions themselves depend on the location of the probe because density of surfactant or water is probe dependent. This makes a quantitative evaluation of detailed dynamics a prohibitively difficult task. However, one can make some progress because of the separation of time scales among the processes that are involved. Since the diffusion of the probe is a slow process, one may approximate the solvation time correlation function by

$$< E(0)E(t) > = \int dx P(X,t) < E(X,0)E(E(X,t) >, \quad (8)$$

where P(X,t) gives the time evolution of the probe's location. A semi-quantitative description of the dynamics of the above process can be achieved by using a Smoluchowski level description where the probability distribution of the solute probe may follow the following equation of motion

$$\frac{\partial P}{\partial t} = D\frac{\partial^2}{\partial X^2}P - \frac{D}{kT}\frac{\partial}{\partial X}(FP) \quad (9)$$

where the force F is due to the potential gradient felt by the solute dipole created by the optical excitation. This equation gives the time scale of the evolution of the probability distribution under the force field. The initial and the final distributions are obviously different and are given by

$$P_0(X,t) = n_0 \exp(-\beta V_0(X)), \quad (10)$$

$$P_{Eq}(X) = n_0 \exp(-\beta V_{Eq}(X)). \quad (11)$$

The initial and final potentials can in principle be calculated from the density functional theory outlined above but that is still rather hard. A simple way to express the potential V is to invoke a continuum model with a space depend-

ent dielectric constant ε(X) (see Fig. 2). The potential energy at a position X of an ionic probe can then be crudely approximated by

$$V(X) \cong -q^2 / a[1-1/\varepsilon(X)] \quad (12)$$

The solvation dynamics probed will then be determined by the diffusion of the probe from lower to the larger dielectric constant. Inside the hydrophobic core, the dielectric constant can be small, about 3-5, while in the bulk, it is close to 80. The radius *a* is about 3-5 Å. The Smoluchowski equation can now be solved to obtain the following expression

$$\tau_s(X_0, b) = \frac{1}{D}[\int_{X_0}^{X_M} dy \exp(\beta V(y)) \int_b^y dz \exp(-\beta V(z)]. \quad (13)$$

where $\beta = 1/k_BT$. X_0 is the starting position, X_M is the final position and b is a position left of X_0 where probability is zero. Therefore, the average time is integration over the initial probability distribution, $P_0(X)$. The position b could be taken as at 4-6 Å inside the initial position of the probe inside the micelle. D is an average diffusion constant which should in principle also have an X dependence which is neglected here for simplicity. Typically viscosity in the core is expected to be about twice that of liquid water.

If one assumes that the probe is a sphere of radius *a* = 3 Å, the partial charge created on the probe at t = 0 is 0.5 esu, the probe diffuses as distance of 4*a* with an average diffusion coefficient of 10^{-5} cm^2/sec, then one obtains an estimate of 740 ps from the above expressions. Evidently, in spite of its simplicity this model gives an estimate of the time scale which is close to that observed in many experiments.

COMPUTER SIMULATION STUDIES

The microscopic details of dynamics of a water molecule at the surface of a micelle and a protein has recently been delineated by detailed atomistic molecular dynamics (MD) simulations. In this section, we briefly summarize some of our most recent results. In these simulations, we used classical, non-polarizable force fields. We present results on a protein HP-36 (subdomain of chicken villin head piece). We also discuss results on two micelles-cesium perflurooctanoate (CsPFO) and decyltrimethylammonium bromide (DeTAB).

Reorientational and Solvation Dynamics of Water Molecules Around a Protein

The rotational motion of water can be investigated by measuring the reorientational dynamics of its electrical dipole μ, defined as the vector connecting the oxygen atom of the water molecule to the center of the line connecting the two hydrogen atoms. The time evolution of μ may be estimated by measuring the dipole-dipole time correlation function (TCF), defined as

$$\boldsymbol{C}_\mu(\boldsymbol{t}) = \frac{\langle \mu_i(\boldsymbol{t}).\mu_i(0) \rangle}{\langle \mu_i(0).\mu_i(0) \rangle} \quad (14)$$

where $\mu_i(t)$ is the dipole moment vector of *i*th water molecule at time t, and the angular brackets denote time averaging over the trajectory of the water molecules, as well as over the initial configurations, $\mu_i(0)$.

In Fig. 7, we show the variation of $C_\mu(t)$ against time for the water molecules near the three helices of the protein, HP-36.[17] For comparison, we have also shown the relaxation for bulk water. The extraordinary slow decay for the helix-2 suggests the presence of a small fraction of 'bound' water molecules near the surface of the helix.

In Fig. 8, we show solvation time correlation function $C_S(t)$ for the polar amino acid residues of the three α-helices of the HP-36 protein.[17] We have calculated $C_S(t)$ by measuring the polar part of the interaction energy between the polar amino acid residues of each of the three helices of the protein and the rest of the system. The decay of solvation TCFs clearly shows the presence of a significantly slow component for all three helices, which is in good

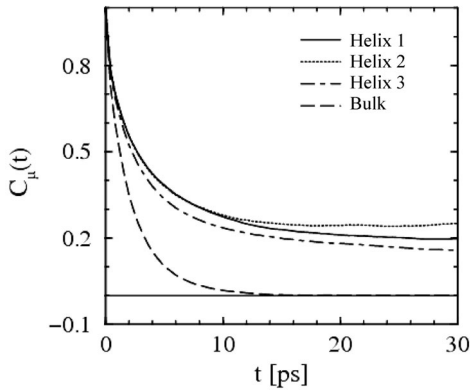

Fig. 7. Dipolar time correlation function of the water molecules, $C_\mu(t)$, for the water molecules in proximity to three α-helices of the HP-36 protein. The TCF for the bulk water is shown for comparison (ref. 17).

agreement with time-resolved fluorescence studies. In HP-36, the initial ultrafast relaxation arises from the high frequency librational (hindered rotation) and intermolecular vibrational (hindered translation) motions of the 'free' or bulk-like water molecules. The moderately damped rotational motions of these water molecules contribute to the fast relaxation (~1 ps). The slowest component observed (42-88 ps) arises from those water molecules which are 'quasi-bound' to the amino acid residues of the protein molecule by strong hydrogen bonds.[17] Interestingly, we notice that the $C_S(t)$ curve decays much faster for helix-2, compared to the other two helices. There could be several factors responsible for this, such as the relative hydrophilicity of the polar amino acid residues present in the three helices and their relative exposure to the solvent, the life-time of the hydrogen bonds between the 'bound' water molecules and the protein residues and the side chain motion of the residues.[17]

Reorientation, Solvation Dynamics and Dielectric Relaxation in a Micelle

Fig. 9 displays the single particle dipolar orientational relaxation [$C_\mu(t)$] of interfacial water molecule in two micelles (CsPFO and DTAB) along with the corresponding relaxation dynamics in bulk water. The interfacial water molecules are defined as those which are within the first coordination shell of head group carbon (for CsFPO micelle) or head group nitrogen (for DTAB micelle). It is apparent that compared to bulk water the dynamics in the micelles is markedly slower. The interfacial water molecules in the CsPFO micelles display slower orientational relaxation compared to DTAB micelles. This could be due to the hydrogen bonding of the water molecules with the polar head group (PHG) of the CsPFO micelle, which is not possible for a DTAB micelle.

Solvation dynamics of the bromide ions in a DTAB micelle at 300 K is shown in Fig. 10. The insets show for both cases the same function for counter ions in neat water at 300 K. In this case, the decay of the solvation TCF is highly nonexponential and one needs a sum of at least three exponentials to fit the solvation TCF. The average solvation time is slower by about a factor of 20 than the corresponding value in the bulk for both cases. However, the long time decay is slower by more that two orders of magnitude, in agreement with the experimental results. The analysis of the partial solvation TCF (not shown here) in the micelles indicate that the contribution from the polar interaction of the cesium ion and bromine ion with the micelle head groups is the most dominant factor. The partial time correlation function exhibits a very slow component which is the leading cause for the slow decay of the total solvation.

Dielectric relaxation (DR) experiments measure the collective polarization response of all the polar molecules

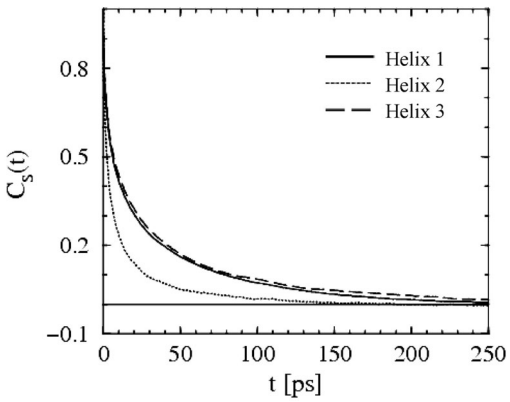

Fig. 8. The solvation time correlation function $C_S(t)$ for the polar amino acid residues of the three α-helices of the HP-36 protein (ref. 17).

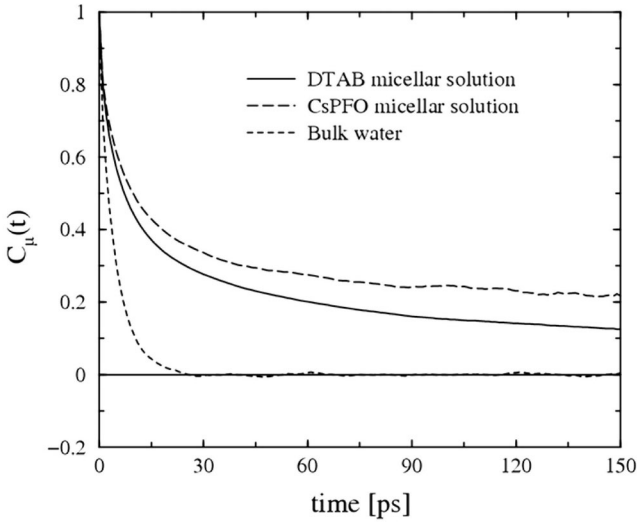

Fig. 9. Dipole-dipole time correlation function [$C_\mu(t)$] for the interfacial water molecules both in the CsPFO micellar solution (long dashed line) and DTAB micellar solution (continuous line). TCF for the bulk water is show for comparison (short dashed line). For details, (ref. 16).

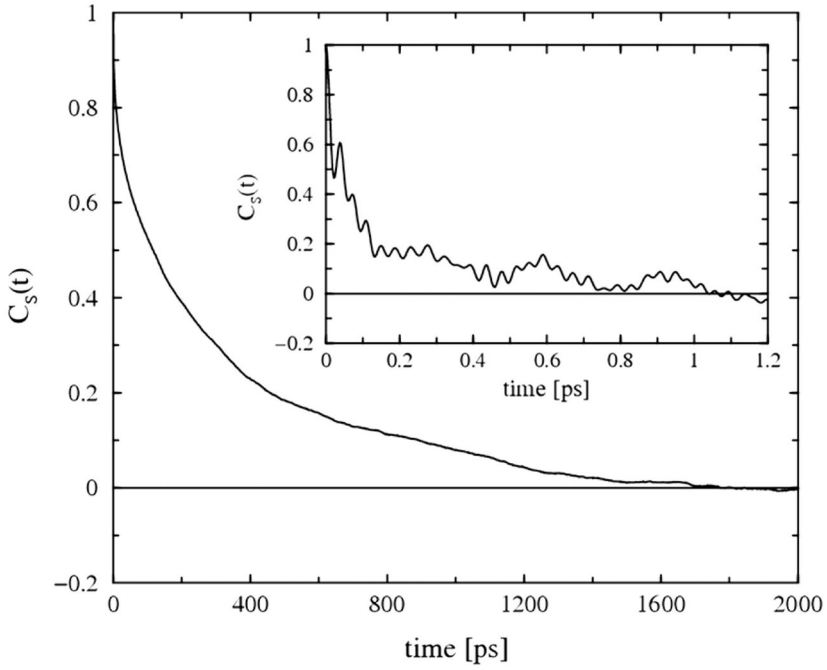

Fig. 10. Solvation time correlation function, $C_S(t)$, for bromine ions in the DTAB micellar solution at 300 K. Inset shows the same for bromine ion in pure water (ref. 18).

present in a given system. The dielectric relaxation time provides a measure of the time taken by a system to reach the final (equilibrium) polarization after an external field is suddenly switched on (or off). DR measures the complex dielectric function, $\varepsilon(\omega)$, that can be decomposed into real and imaginary parts as $\varepsilon(\omega) = \varepsilon'(\omega) - i\varepsilon''(\omega)$ where $\varepsilon'(\omega)$ and $\varepsilon''(\omega)$ are the real (permittivity factor) and imaginary (dielectric loss) parts respectively.

We have calculated the total moment-moment TCF of water (only), both in the presence (solid line) and in the absence of the CsPFO micelle in the simulation box, i.e., in bulk or neat water.[18] The TCF was fitted to a multi-exponential form to get the time constants and amplitudes which can be used to calculate the frequency dependent dielectric constant. The simulations show the presence of a slow component with a time constant of 41 ps, in contrast to a value of only 9 ps for bulk water. The presence of the 41 ps component in the dielectric relaxation of the micellar water can be traced back to the dynamic exchange of water molecules between its bound and free states at the interface.[8] The Cole-Cole plot shown in Fig. 11 shows considerable degree of nonexponentiality in the dielectric spectrum.[18]

CONCLUDING REMARKS

The recent experimental studies using time resolved

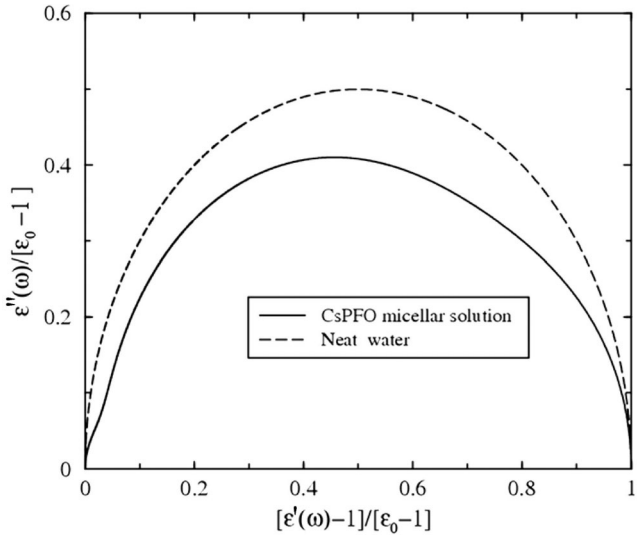

Fig. 11. Cole-Cole plot of the frequency dependent dielectric function, where the imaginary part, $[\varepsilon''(\omega)]/[\varepsilon_0\text{-}1]$ is plotted against the real part, $[\varepsilon'(\omega)\text{-}1]/[\varepsilon_0\text{-}1]$, for the water molecules, both in CsPFO micellar solution (solid line) and in the neat water (dashed line) (ref. 18).

fluorescence techniques as well as computer simulations and theoretical studies have considerably improved our understanding of dynamics in complex biological systems. This article gives a brief overview on the insight gained recently into the dynamics in different biological and self-assembled systems. The above analysis suggests that in some cases, there could be more than one mechanism that can give rise to an ultraslow component observed in recent experiments and the relative contributions may be hard to estimate. One could, however, roughly estimate the time scales responsible for the different slow mechanisms. It is clear that the dynamic exchange between the free and the bound states of water molecules at the surface is important at relatively short times. The temperature variation study supports the dynamic exchange model and may be used to estimate the activation energy and entropy of activation for solvation dynamics. Self-diffusion of the probe may contribute next in order of time scale, and its time scale depends on the width of the hydrophobic core that the probe needs to diffuse through. The role of the self-diffusion of the probe could be estimated by the variation of the width Γ at half-maximum of TRES. Finally, we show that the model of cooperative chain melting may give rise to an ultraslow component of solvation dynamics.

Received June 2, 2005.

ACKNOWLEDGEMENT

This work was supported by the Department of Science and Technology and the Council of Scientific and Industrial Research, government of India. We thank Prof. Balasubramanian for collaboration.

REFERENCES

1. Jimenez, R.; Fleming, G. R.; Kumar, P. V.; Maroncelli, M. *Nature* **1994**, *369*, 471.
2. Nandi, N.; Roy, S.; Bagchi, B. *J. Chem. Phys.* **1995**, *105*, 1390.
3. Fecko, C. J.; Eaves, J. D.; Loparo, J. J.; Tokmakoff, A.; Geissler, P. L. *Science* **2003**, *301*, 1698.
4. Nandi, N.; Bhattacharyya, K.; Bagchi, B. *Chem. Rev.* **2000**, *100*, 2013.
5. Bhattacharyya, K. *Acc. Chem. Res.* **2003**, *36*, 95.
6. Bagchi, B. *Annu. Rep. Prog. Chem. Sect. C* **2003**, *99*, 127.
7. Bhattacharyya, K.; Bagchi, B. *J. Phys. Chem. B* **2000**, *104*, 10603.
8. Nandi, N.; Bagchi, B. *J. Phys. Chem. B* **1997**, *101*, 10954.
9. Jordanides, X. J.; Lang, M. J.; Song, X.; Fleming, G. R. *J. Phys. Chem. B* **1999**, *103*, 7995.
10. Mandal, D.; Sen, S.; Sukul, D.; Bhattacharyya, K.; Mandal, A. K.; Banerjee, R.; Roy, S. *J. Phys. Chem. B* **2002**, *106*, 10741.
11. Vajda, S.; Jimenez, R.; Rosenthal, S. J.; Fidler, V.; Fleming, G. R.; Castner, E. W. Jr. *J. Chem. Soc. Faraday Trans.* **1995**, *91*, 867.
12. Andreatta, D.; Louis Pérez Lustres, J.; Kovalenko, S. A.; Ernsting, N. P.; Murphy, C. J.; Coleman, R. S.; Berg, M. A. *J. Am. Chem. Soc.* **2005**, *127*, 7270.
13. Sen, P.; Mukherjee, S.; Halder, A.; Bhattacharyya, K. *Chem. Phys. Lett.* **2004**, *385*, 357.
14. Dutta, P.; Sen, P.; Mukherjee, S.; Halder, A.; Bhattacharyya, K. *J. Phys. Chem. B* **2003**, *107*, 10815.
15. Balasubramanian, S.; Pal, S.; Bagchi, B. *J. Phys. Chem. B* **2003**, *107*, 5194.
16. Pal, S.; Balasubramanian, S.; Bagchi, B. *J. Chem. Phys.* **2004**, *120*, 1912.
17. Bandyopadhyay, S.; Chakraborty, S.; Balasubramanian, S.; Bagchi, B. *J. Am. Chem. Soc.* **2005**, *127*, 4071.
18. Pal, S.; Bagchi, B.; Balasubramanian, S. *J. Phys. Chem. B* **2005**, in press.
19. Faeder, J.; Ladanyi, B. M. *J. Phys. Chem. B* **2005**, *109*, 6732.
20. Levitt, M.; Sharon, R. *Proc. Natl. Acad. Sci. USA* **1988**, *85*, 7557.
21. Pasenkiewicz-Gierula, M.; Takaoka, V.; Miyagawa, H.; Kitamura, K.; Kusumi, A. *J. Phys. Chem. A* **1997**, *101*, 3677.
22. Allen, R.; Bandyopadhyay, S.; Klein, M. L. *Langmuir* **2000**, *16*, 10547.
23. Bandyopadhyay, S.; Chanda, J. *Langmuir* **2003**, *19*, 10443.
24. Guha, S.; Sahu, K.; Roy, D.; Mondal, S. K.; Roy, S.; Bhattacharyya, K. *Biochemistry* **2005**, in press.
25. Sen, P.; Mukherjee, S.; Dutta, P.; Halder, A.; Mandal, D.; Banerjee, R.; Roy, S.; Bhattacharyya, K. *J. Phys. Chem. B* **2003**, *107*, 14563.
26. Dutta, P.; Sen, P.; Halder, A.; Mukherjee, S.; Sen, S.; Bhattacharyya, K. *Chem. Phys. Lett.* **2003**, *377*, 229.
27. Sen, P.; Roy, D.; Sahu, K.; Mondal, S. K.; Bhattacharyya, K. *Chem. Phys. Lett.* **2004**, *395*, 58.
28. Sen, P.; Mukherjee, S.; Patra, A.; Bhattacharyya, K. *J. Phys. Chem. B* **2005**, *109*, 3319.

29. Satoh, T.; Okuno, H.; Tominaga, K.; Bhattacharyya, K. *Chem. Letts.* **2004**, *33*, 1090.
30. Sen, P.; Satoh, T.; Tominaga, K.; Bhattacharyya, K. *Chem. Phys. Lett.* **2005**, in press.
31. Wand, A. J.; Ehrhardt, M. R.; Flynn, P. F. *Proc. Natl. Acad. Sci. (USA)* **1998**, *95*, 15299.
32. Dutta, P.; Sen, P.; Mukherjee, S.; Bhattacharyya, K. *Chem. Phys. Lett.* **2003**, *382*, 426.
33. Pal, S. K.; Datta, A.; Mandal, D.; Bhattacharyya, K. *Chem. Phys. Lett.* **1998**, *288*, 793.
34. Sen, S.; Sukul, D.; Dutta, P.; Bhattacharyya, K. *J. Phys. Chem. A* **2001**, *105*, 7495.